Journal of Inorganic Biochemistry 138 (2014) 9–15

Contents lists available at ScienceDirect

Journal of Inorganic Biochemistry

journal homepage: www.elsevier.com/locate/jinorgbio

Proton and gallium(III) binding properties of a biologically active salicylidene acylhydrazide

Shoghik Hakobyan, Jean-François Boily *, Madeleine Ramstedt **

Department of Chemistry, Umeå University, 901 87 Umeå, Sweden

ARTICLE INFO

Article history:
Received 3 February 2014
Received in revised form 14 April 2014
Accepted 15 April 2014
Available online 29 April 2014

Keywords:
Protonation
Complex formation
Gallium
pH titration
UV–VIS
Equilibrium constants

ABSTRACT

Bacterial biofilm formation causes a range of problems in our society, especially in health care. Salicylidene acylhydrazides (hydrazones) are promising antivirulence drugs targeting secretion systems used during bacterial infection of host cells. When mixed with the gallium ion they become especially potent as bacterial and biofilm growth-suppressing agents, although the mechanisms through which this occurs are not fully understood. At the base of this uncertainty lies the nature of hydrazone–metal interactions. This study addresses this issue by resolving the equilibrium speciation of hydrazone–gallium aqueous solutions. The protonation constants of the target 2-oxo-2-[*N*-(2,4,6-trihydroxy-benzylidene)-hydrazino]-acetamide (ME0163) hydrazone species and of its 2,4,6-trihydroxybenzaldehyde and oxamic acid hydrazide building blocks were determined by UV–visible spectrophotometry to achieve this goal. These studies show that the hydrazone is an excessively strong complexing agent for gallium and that its antivirulence properties are predominantly ascribed to monomeric 1:1 Ga–ME0163 complexes of various Ga hydrolysis and ME0163 protonation states. The chelation of Ga(III) to the hydrazone also increased the stability of the compounds against acid-induced hydrolysis, making this group of compounds very interesting for biological applications where the Fe-antagonist action of both Ga(III) and the hydrazone can be combined for enhanced biological effect.

1. Introduction

As traditional antibiotics are becoming increasingly inefficient, new approaches in treating bacterial infections are needed. Drugs that target virulence factors are one of such routes, disabling pathogens to infect a host and cause disease. Anti-virulence drugs would protect from disease by disarming but not killing the pathogen. Such a strategy attenuates the selective pressure for development of drug resistance compared to biocides [1]. Salicylidene acylhydrazides—known as hydrazones—are highly promising anti-virulence components, inhibiting type III secretion system in a range of Gram-negative bacteria [2] without killing them. Although virulence-inhibiting mechanisms of hydrazones are largely unknown, recent studies are pointing to multiple targets in the bacterial cell [2,3].

The hypothesis of hydrazone binding to the trivalent Fe(III) and Ga(III) ions has also received much attention in the literature due to its possible work in depleting the solution of bioavailable Fe [4–9]. In order to compare the chelating efficiency of hydrazones and siderophores, equilibrium constants are very important. Unfortunately, very little thermodynamic data exists on hydrazone–metal ion affinity, thus impeding the advancement of knowledge in this area. In a study by Richardson et al., three acidity constants (pK_a) were obtained for a substance of similar structure (Fig. 1b). They found three pK_a values of 3.43 (pyridyl nitrogen), 8.29 (sole hydroxyl group on benzyl ring) and 9.8 (the ═N–NH– hydrogen of the hydrazone motif) [7]. In the presence of Fe this ligand (L) was found to form four Fe complexes with overall formation constants ($\log \beta_{pqr}$) of $\log \beta_{-1,1,1} = 38.3$ ($FeHL^{2+}$), $\log \beta_{-2,1,2} = 48.8$ ($Fe(HL)_2^+$), $\log \beta_{-3,1,2} = 54$ ($Fe(HL)L^0$) and $\log \beta_{-4,1,2} = 56$ (FeL_2^-). These formation constants would result in a free Fe concentration of 10^{-50} M (i.e. $-\log[Fe^{3+}] = pFe = 50$) in a solution with pH 7.4, $[Fe(III)] = 10^{-6}$ M and $[L] = 10^{-3}$ M [8], showing that this group of substances can be very strong Fe chelators, in fact stronger than many bacterial siderophores (e.g. enterobactin result in pFe = 38 and desferrioxamin B (DFOB) pFe = 28, pyoverdin pFe = 28 under similar conditions [8,10]) as well as mammalian Fe-binding proteins transferrin and lactoferrin. However, protonation and binding to metal ions can vary between molecules in the hydrazone family due to substituents in the molecule [7,8,11], giving rise to differences in hydrophilicity and lipophilicity [11] or electron distribution [12].

Restriction of iron to bacteria can also be achieved through the use of Ga(III), an Fe(III) mimetic that is taken up into the bacterial cells via Fe(III) uptake routes using bacterial siderophores [13]. Ga(III) can inhibit biofilm formation and growth especially for bacteria with high

* Corresponding author. Tel.: +46 90 786 5270; fax: +46 90 786 7655.
** Corresponding author. Tel.: +46 90 786 6328; fax: +46 90 786 7655.
E-mail addresses: jean-francois.boily@chem.umu.se (J.-F. Boily), madeleine.ramstedt@chem.umu.se (M. Ramstedt).

http://dx.doi.org/10.1016/j.jinorgbio.2014.04.012

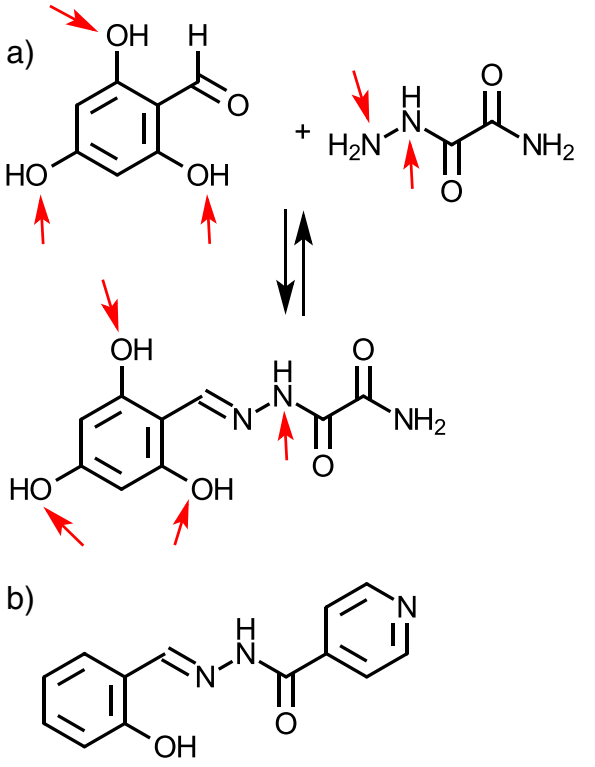

Fig. 1. a) Synthesis of ligand 2-oxo-2-[N-(2,4,6-trihydroxy-benzylidene)-hydrazino]-acetamide (ME0163 or L) from the 2,4,6-trihydroxybenzaldehyde (THB) and oxamic acid hydrazide (OAH). Arrows show protonation sites (here neutral forms of substances are shown). b) Hydrazone in Richardson et al. [7,8].

demands for Fe [13–15] such as *Pseudomonas aeruginosa*, supposedly, by being incorporated into bacterial metabolic systems that demand iron and, subsequently, disrupting them [16]. Additionally, chelation with gallium ions [12,17,18] has been shown to enhance the effect of hydrazones that target Fe metabolism in tumors and was proposed as candidates for anti-cancer drugs [19,20] suggesting that the same could be true for effects on bacterial cells. These findings are thereby calling for an understanding of the nature of hydrazone–gallium interactions in aqueous solutions, which is the object of this study. The equilibrium stability constants of hydrazone–gallium complexes were determined for the ME0163 ligand (Fig. 1a), a complex that in a parallel study was found to have high anti-biofilm and anti-virulence properties [21]. The speciation of the ligand and Ga(III) complex was resolved by UV–visible (UV–VIS) spectrophotometric measurements of solutions at various Ga(III):ligand ratios, in part due to the low solubility of this ligand. A chemometric treatment of the resulting spectral sets was used to extract stability constants for its protonation constants and gallium-binding constants. These efforts also extracted molar absorption coefficients that can be used to identify various hydrazone species in subsequent studies.

2. Methods

2.1. Chemicals

Chemicals were purchased from Sigma-Aldrich and used without purification unless otherwise stated. The 2-oxo-2-[*N*-(2,4,6-trihydroxy-benzylidene)-hydrazino]-acetamide (ME0163) hydrazone was synthesized (Fig. 1) by a method described elsewhere [2] using 2,4,6-trihydroxybenzaldehyde (THB) (Aldrich) and oxamic acid hydrazide (OAH) (Acros Organics) as parent building blocks. The molecular structure of ligand ME0163 used in this study was confirmed NMR. All solutions were prepared from deionized and boiled water (resistance = 18.2 MΩ) at an ionic strength of 0.1 M NaCl (Merck p.a., dried at 453 K). A 30 mM HCl solution in 0.1 M NaCl was made from concentrated HCl (37% Aldrich) and standardized against tris(hydroxymethyl) aminomethane (Trizma base). A 10 mM NaOH solution in 0.1 mM NaCl (degassed with N_2(g)) was made from a 50% NaOH solution and standardized against the standardized HCl solution. A 10.6 mM $Ga(NO_3)_3$ solution was prepared from $Ga(NO_3)_3.xH_2O$ (Aldrich) in 0.1 M NaCl and 40.5 mM NaOH, giving gallium in the form of the soluble $Ga(OH)_4^-$ ion. The exact concentration of Ga(III) ions was determined by using Atom Absorption Spectrometry (Perkin Elmer AAS 3110).

2.2. NMR

NMR analyses at low pH 1.5–4.0 were carried out using a Bruker (400 MHz) NMR spectrometer in D_2O:H_2O (~99:1). The samples (~1 mM) were prepared by adding 10 mM NaOH solution into the solution of ME163 ligand (L) in 0.1 M NaCl, and pH was adjusted by 30 mM HCl. In case of the Ga(III)–L system, 10.6 mM $Ga(OH)_4^-$ solution was also added. The samples were equilibrated overnight (~16 h).

2.3. UV–VIS spectrophotometric titrations

Protonation constants of the parent 2,4,6-trihydroxybenzaldehyde (THB), parent oxamic acid hydrazide (OAH), and synthetic ME0163 hydrazone species were determined by UV–VIS spectrophotometric titrations [22–24]. Ga(III)-binding constants to ME0163 were also determined using the same method. Due to the low solubility of hydrazones and the sensitivity range in the UV–VIS spectrophotometer, very dilute solutions of [L] = 0.034–0.063 mM and [Ga] = 0.052–0.074 mM were used. Experiments were done with ratios L:Ga = 1:1.2 and 1:1.3. The concentrations were determined by careful gravimetric measurements of dry hydrazone before dissolution into a well-determined volume of ionic medium. The concentrations were double checked using a calibration curve made by diluting a solution at relatively high concentration (1.35 mM) and creating a calibration curve from UV–VIS spectra. Concentration range for the calibration curve was 0.07–0.02 mM. More detailed description for the titrations can be found in supplementary information.

2.4. Speciation calculations

Experimental data obtained from potentiometric titration and UV–VIS measurements were used for thermodynamic and spectrophotometric predictions of the speciation of the THB, OAH and ME0163 ligands (H_sL, where s is 3, 1 and 4 respectively). Mass action equations are expressed for the L complexes as:

$$H_{s+p}L_r^{\,p} \rightleftharpoons pH^+ + rH_sL \tag{1}$$

where $K_a \cdot [H_{s+p}L_r]^{\,p} = [H_sL^0]^r \cdot [H^+]^p$ and for Ga(III)–H_4L with:

$$pH^+ + qGa^{3+} + rH_4L \rightleftharpoons Ga_q(H_4L)_r(H)_p^{\,3q+p} \tag{2}$$

where $[Ga_q(H_4L)_r(H)_p]^{3q+p} = \beta_{p,q,r} \cdot [H^+]^p \cdot [Ga^{3+}]^q \cdot [H_4L^0]^r$

Mass balance equations are:

$$[Ga]_{Tot} = \sum_0^p \sum_0^q \sum_0^r q\left[Ga_q(H_4L)_r(H)_p\right]^{3q+p} \tag{3}$$

$$[L]_{Tot} \sum_0^p \sum_0^q \sum_0^r r\left[Ga_q(H_4L)_r(H)_p\right]^{3q+p} \tag{4}$$

$$[H]_{Tot} = \sum_0^p \sum_0^q \sum_0^r p\left[Ga_q(H_4L)_r(H)_p\right]^{3q+p} + \left[H^+\right] - K_w^{-1}\left[H^+\right]^{-1} \tag{5}$$

In these expressions, *p*, *q* and *r* are stoichiometric coefficients. The chloride and sodium ion mass balances were not considered in the

calculations as all experiments were carried out in a constant ionic medium. Description of how spectrophotometric data were related to the thermodynamic models can be found in supplementary information.

Molar absorption coefficients and stability constants were first determined for the building block THB and OAH molecules. These values were then used in the evaluation of the stability constants of ME0163 to address possible spectral contributions from the building blocks appearing by hydrolytic cleavage at low pH whereby:

$$ME0163 + H_2O + H^+ \rightleftharpoons THB^0 + HOAH^+ \quad (6)$$

Possibilities for gallium-oxyhydroxide precipitation were also taken into account in the modeling procedure by determining the total gallium solubility in the ME0163-bearing system.

2.5. Molecular modeling

Lowest energy conformers as well as pKa values of ME0163 and both parent compounds were identified using MarvinSketch 6.1.3 (ChemAxon [26]). Energy calculations were carried out using the Merck Molecular Force Field 94 (MMFF94), using very strict optimization limits defined by the program. Molecular energies were calculated for all possible protonation configurations; pKa values were predicted using macro mode and dynamic acid/base prefix.

3. Results and discussion

3.1. Protonation of ME0163 and of its parent compounds

A prerequisite to determining gallium–ME0163 binding strength entails knowledge of the stability field of the ligand as well as its protonation constants. Potential protonation sites for the parent compounds and the ligand are indicated in Fig. 1a. pKa values for these protonation sites (Table 1) were first estimated using MarvinSketch 6.1.3 to guide interpretations of experimental data. Protonation constants of hydroxyl groups (7.48 *ortho*, 8.98 *ortho*, 10.3 *para*) and amino groups (2.25 NH–$\underline{NH_3^+}$, 10.2 CO–NH) for parent compounds are somewhat comparable to those of the ME0163 ligand (8.54, 9.72, 10.7 for *ortho*-, *ortho*-, *para*-hydroxyl groups; 11.3 for the N–NH bridge).

In an effort to facilitate the experimental determination of pKa values of ME0163, the protonation constants of the three phenolic OH groups of the parent THB molecule were first determined. The UV–VIS spectra of THB are characterized by strong π–π* transitions involving phenyl ring p-orbitals as well as charge-transfer-to-solvent (CTTS) transitions of the basic phenolic oxygen lone pairs hydrogen-bonded to solvent water molecules (Fig. 2a). A strong peak at 320 nm in alkaline solutions gradually attenuates with acidity and ultimately gives rise to a predominant peak at 290 nm in acidic solutions. A singular value decomposition (SVD)-based dimensional analysis points to the contribution of 4 linearly-independent components describing the variance in the absorbance data, corresponding to the THB^{3-}, THB^{2-}, THB^{1-} and THB^0 species. Extraction of the stability constants and molar absorption coefficients of these species using the method described in Section 2.3 gave the equilibrium constants $pK_{a1} = 9.6$, $pK_{a2} = 7.6$, and $pK_{a3} = 5.6$, and fully described the experimental data (Fig. 2b and Table 1). These values were lower than the predicted values. The resulting molar absorption coefficients show that the first two protonation steps correspond to considerable attenuations of the 320 nm peak, while the last with a strong blue shift to 290 nm. This last shift thus corresponds to the formation of a neutrally-charged species, and thus to decreased CTTS transitions undergone by the charged species at the lower energy 320 nm peak.

The same exercise was repeated for the OAH building block of ME0163 (Fig. 2c and d). The lower level of conjugation in this molecule gives rise to less complex UV–VIS spectra, shifted towards higher energy values. In this case, a peak at 275 nm becomes largely attenuated by protonation, leaving a faint shoulder at 250 nm of superimposed on stronger portion of a peak gaining importance at wavelengths below 226 nm. All data can be fit by two species related by the $pK_{a1} = 10.1$, one that it associated to the protonation of the basic N group of this molecule. The corresponding OAH^- species has thus a strong discernable peak at 275 nm due to CTTS transitions involving the N lone pair, which then attenuates in OAH^0. This pKa agreed well with the predicted pKa value. However, the additional protonation step predicted at low pH could not be resolved experimentally.

The ME0163 ligand exhibits comparable traits to THB, except that its lowest energy peak is ~47 nm lower (Fig. 3). This effect is the possible result of the increased electron delocalization in the ME0163 coupled with its greater charge. The 380 nm peak undergoes a strong attenuation with protonation, blue-shifting by ~47 nm to 333 nm by pH 5.1 then ultimately to ~290 nm at pH 3.1, just as in THB. Given possible complications arising from the hydrolytic cleavage of CH═N in aqueous solution, producing the original parent molecules, UV–VIS and NMR spectra were first surveyed over a broad range of solution conditions. These efforts notably showed that the ligand did decompose at pH below ~3.7, as can be seen by the disappearance of –CH═N– (8.36 ppm) and concomitant appearance of –CH═O moiety (9.90 ppm) below this value in NMR spectra (Fig. 4). Spectrophotometric titrations also showed that this reaction was reversible, and could be described as a proton-promoted hydrolytic cleavage of ME0163 to the THB^0 and the protonated form of OAH^0, as described in Eq. (6).

Having identified the pH stability fields of the ME0163 ligand, the corresponding spectrophotometric data were used to extract protonation constants for this ligand. A dimensionality analysis pointed to five linearly-independent components. One of these components corresponds to THB^0, with a peak at 290 nm while the one from OAH^0 could not be clearly elucidated given its relatively low intensities. The remaining four components thereby correspond to three protonation steps in ME0163. Extraction of proton-promoted hydrolytic cleavage (K_{HC}) and protonation constants was carried out using molar absorption coefficients of the parent molecules as hard constraints. Best-fitting protonation constants (Table 1) are comparable to those of the parent THB species, suggesting that the first (pK_{a1} (H_4L) = 6.8; pK_{a2}(H_3L) = 7.7) correspond to the deprotonation of phenolic groups. The third deprotonation may originate from the remaining phenolic group or the N–NH bridge, and based on the pKa predictions we assign it to the phenol in *para*- position. Note that distinct protonation constant for the last protonation step could not be extracted from the data as it is expected at pH >11. The assignment is also supported by molecular energy

Table 1
Equilibrium constants for $Ga_q(H_4L)_r(H)_p^{3q+p}$ describing the protonation of starting materials (2,4,6-trihydroxybenzaldehyde (THB) and oxamic acid hydrazide (OAH)), ligand ME0163 and Ga(III)–ME0163 complex in solutions at 25 °C and I = 100 mM.

Systems	*p,q,r*	Products	$\log\beta_{p,q,r}$	pKa's from exp/theory
THB (H_3L)	1,0,1[a]	H_2L^{1-}	−5.6	5.6/7.48
	2,0,1[a]	HL^{2-}	−13.2	7.6/8.98
	3,0,1[a]	L^{3-}	−22.8	9.6/10.3
OAH (HL)	1,0,1[a]	L^{1-}	−10.1	10.1/10.2
	−1,0,1[a]	H_2L^+		-/2.25
ME0163 (H_4L)	1,0,1[a]	H_3L^{1-}	−6.8	6.8/8.54
	2,0,1[a]	H_2L^{2-}	−14.5	7.7/9.72
	3,0,1[a]	HL^{3-}	−25.1	10.6/10.7
	4,0,1[a]	L^{4-}	-	-/11.3
	HC[c]	$HOAH^+ + THB$	1.2	
Ga(III)–ME0163	−3,1,1[b]	$[Ga(OH)_2H_3L]^0$	32.8	
	−4,1,1[b]	$[Ga(OH)_3H_3L]^{1-}$	29.4	
	−6,1,1[b]	$[Ga(OH)_3HL]^{3-}$	16.1	

[a] Stoichiometric coefficients for the protonation of the ligands (Eq. (1)).
[b] Stoichiometric coefficients for Ga–ME0163 complexation (Eq. (2)).
[c] Constant for hydrolytic cleavage (Eq. (6)). The hydrolysis constants for Ga^{3+} are [25]: $\log\beta_{-1,1,0} = -3.93$; $\log\beta_{-2,1,0} = -7.73$; $\log\beta_{-3,1,0} = -12.38$; $\log\beta_{-4,1,0} = -15.96$; $\log\beta_{-32,13,0} = -66.3$; $\log\beta_{-3,1,0}(s) = -3.54$.

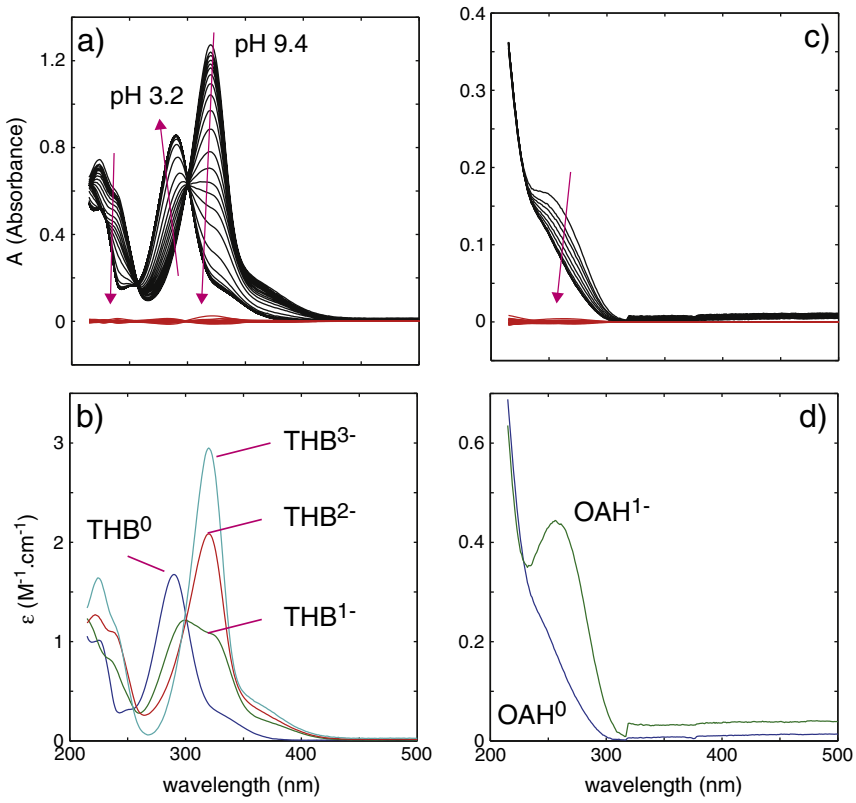

Fig. 2. a and c) Spectrophotometric titrations of a) THB in 0.1 M NaCl at 25 °C in the pH 9.3–3.2 range and c) OAH in 0.1 M NaCl at 25 °C in the pH 10.0–3.3 range. Red arrows show changes in spectral intensity with decreasing pH. Red lines show deviations of fit of the model to the data (black lines). b and d) Molar adsorption coefficients of the four species responsible for the data of a) and c) respectively and related with the pK_a values of Table 1.

calculations of the hydrazone with different protonation sites and steps, detailed in Section 3.4 and the predicted pKa values (Table 1). As for the THB starting material the experimentally determined pKa values for the OH groups in the ligand were lower than the predicted ones. While these values are different to those reported by Richardson on a similar substance (experimental: hydroxyl $pK_a = 8.3$ and N-NH bridge $pK_a = 9.8$, predicted: hydroxyl $pK_a = 8.7$ and N-NH bridge $pK_a = 9.9$) [7], our findings may arise from the high level of conjugation in ME0163, and withdrawing electron density from the N base (Fig. 1). Based on the equilibrium constants obtained, H_4L^0, H_3L^{1-} and H_2L^{2-} are the dominant species in the 3–10 pH range. The model also predicts significant levels of hydrolytic cleavage to the parent THB and OAH compounds from the fully protonated H_4L^0 species under acidic conditions only.

3.2. Ga(III)–ME0163 complexation

A survey of the Ga(III)-bearing solutions over a broad range of pH values was carried out to determine the stability field of ME0163. In contrast to the pure ligand system, ligand decomposition takes place at pH values below 3 (Fig. 5), thus suggesting that Ga(III)–ME0163 complexation stabilizes the ligand against hydrolytic cleavage. We also note that Ga(III) increased the solubility of the ligand, two first observations pointing to significant Ga(III)–ME0163 complexation. A third comes from the enhanced Ga(III) solubility, seen through the absence of any turbidity in the solutions through the lack of light scattering that would have otherwise occurred by colloidal gallium hydroxide particles in the 400–800 nm region at circumneutral pH.

Ga(III)–ME0163 complexation was studied in solutions of Ga(III) (0.05–0.07 mM) and ME0163 (0.04–0.06 mM) (Fig. 6a and b). A dimensionality analysis of the spectra revealed that eight orthogonal components were required to fit the two sets of experimental absorbance data. Emphasizing that none of the soluble gallium hydroxide complexes contribute to the absorbance data and that we have identified five ME0163 species in the previous section, three additional species should be invoked to reproduce the variance of the data. Various species combinations of systematically varied *p*, *q*, and *r* in the complex $Ga_q(H_4L)_r(H)_p$ were tested for their ability to reproduce the absorption matrix, one that was evaluated based on $SOS = \Sigma(\mathbf{A}_{calc} - \mathbf{A}_{exp})^2$. The best-fitting combination of species describing the spectrophotometric titration data consists of $[Ga(OH)_2H_3L]^0$ ($p, q, r = -3,1,1$), $[Ga(OH)_3H_3L]^{1-}$ ($p, q, r = -4,1,1$) and $[Ga(OH)_3HL]^{3-}$ ($p, q, r = -6,1,1$). It therefore only consisted of 1:1 Ga:ME0163 complexes of different protonation states. We note that the molar absorption coefficients of (−3,1,1) and (−4,1,1) are highly similar, and blue-shifted by about 25 nm from those of the (−6,1,1) species are. They are therefore likely to arise from ligands of the same protonation state but gallium ions of different hydrolysis state. Furthermore, we considered the protonation steps of the pure ligand system and the hydrolysis of Ga(III) in the absence of ligand. Thus, assignment of (−6,1,1) best corresponds to the $[Ga(OH)_3HL]^{3-}$ species, while (−4,1,1) to $[Ga(OH)_3H_3L]^{1-}$ and (−3,1,1) to $[Ga(OH)_2H_3L]^0$. The corresponding equilibrium reactions for the formation of these three complexes (with log β values in Table 1) are given below:

$$\beta_{-3,1,1} \quad Ga^{3+} + H_4L + 2H_2O \rightleftharpoons [Ga(OH)_2H_3L]^0 + 3H^+ \tag{7}$$

$$\beta_{-4,1,1} \quad Ga^{3+} + H_4L + 3H_2O \rightleftharpoons [Ga(OH)_3H_3L]^- + 4H^+ \tag{8}$$

$$\beta_{-6,1,1} \quad Ga^{3+} + H_4L + 3H_2O \rightleftharpoons [Ga(OH)_3HL]^{3-} + 6H^+ \tag{9}$$

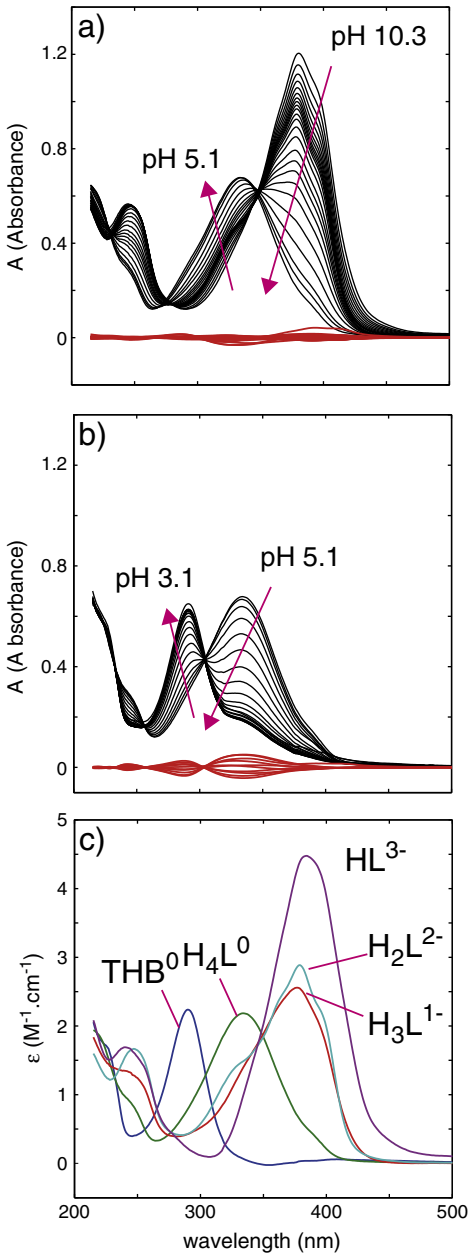

Fig. 3. Spectrophotometric titrations of ME0163 in 0.1 M NaCl at 25 °C in the a) pH 10.3–5.1 and b) pH 5.1–3.2 range. Red arrows show changes in spectral intensity with decreasing pH. Red lines show deviations of fit of the model to the data (black lines). c) Molar adsorption coefficients of the species responsible for the data of a) and related with the pK_a values of Table 1.

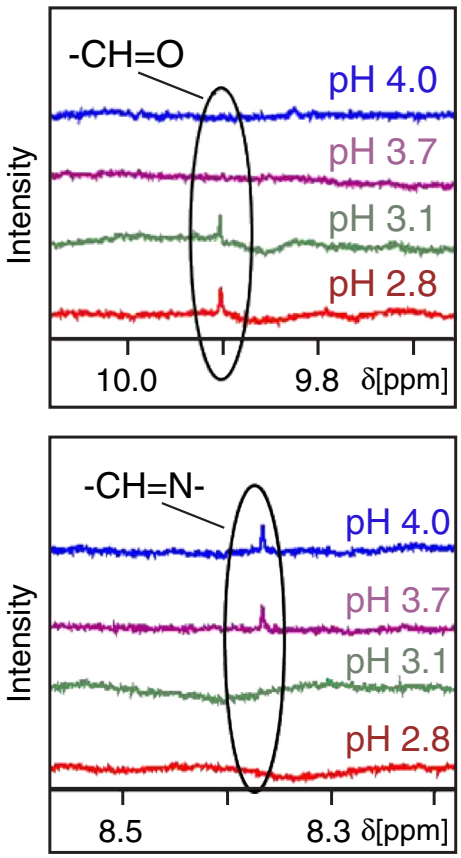

Fig. 4. NMR spectra of ME0163 solutions at pH 2.8, 3.1, 3.7, and 4.0. The data point to the hydrolytic cleavage of –CH═N– of ME0163, producing the THB at pH < < 3.7.

The resulting distribution diagram (Fig. 6c), thus, suggests that at physiological pH the solution predominantly consists of a mixture of the $[Ga(OH)_3HL]^{3-}$ and $[Ga(OH)_3H_3L]^{1-}$ complexes. As for the pure ligand system, the two deprotonation steps of H_3L^- to form HL^{3-} were very close in pH, and could not be separated for the complex. At high pH, the ligand is not complexed and Ga is predominantly in the form of gallate ($Ga(OH)_4^{-1}$). Taking these observations together suggests that Ga(III) should bind in the chelating motive through the azomethine nitrogen, the carbonyl and one phenolic group. Stated otherwise, it is forming both a 5-, and a 6-membered chelate with various moieties of ME0163. These interactions are thus reducing the electron density at the azomethine C–H and N, and thus explaining the downward shift in the NMR spectra from 8.36 ppm in ME0163 to 8.87 ppm in mixed Ga:ME0163 solutions. Finally, we note that these specific interactions are the cause for the greater resilience of ME0163 against the hydrolytic cleavage of CH═N, and hence the persistence of this ligand over a greater range of pH values in the presence of gallium.

3.3. Implications for the biological use of Ga:ME0163

To compare the Ga(III) chelation of this ligand with other relevant ligands, we compared the free gallium ion concentration in the presence of ligand ($-\log[Ga^{3+}] = pGa$) at 1 μM Ga^{3+}, 10 μM ligand and pH 7.4. Ligands that form strong complexes give rise to low free metal ion concentrations, i.e. higher pGa. For the hydrazone in this study pGa was 21.3, for DFOB 25.1, EDTA 21.0 and citrate 19.3 (I = 100 mM). The pGa in water is 18.3 after hydrolysis of Ga^{3+}. This calculation illustrates that the binding strength of the hydrazone to gallium ions is similar to the strong chelator EDTA and a little weaker than the siderophore DFOB that has previously been investigated with Ga(III) for antibacterial purposes [13,14]. This comparison suggests that the complex should be stable in biological media and keep Ga(III) in a soluble bioavailable form. At the same time, since it has a slightly lower affinity compared to bacterial siderophores such as DFOB, it could be expected that Ga(III) would be released from the hydrazone in the presence of siderophores and be taken up into bacterial cells instead of Fe(III) through the Fe(III) uptake routes. Previous studies have shown that Ga(III) complexes with ligands with lower pGa than DFOB (citrate in that study) can more efficiently deliver Ga(III) to the bacterial cells than GaDFOB, presumably since it allows for multiple uptake routes using several siderophores that all have binding affinities similar to that of DFOB [12]. Compared to citrate, the hydrazone in this

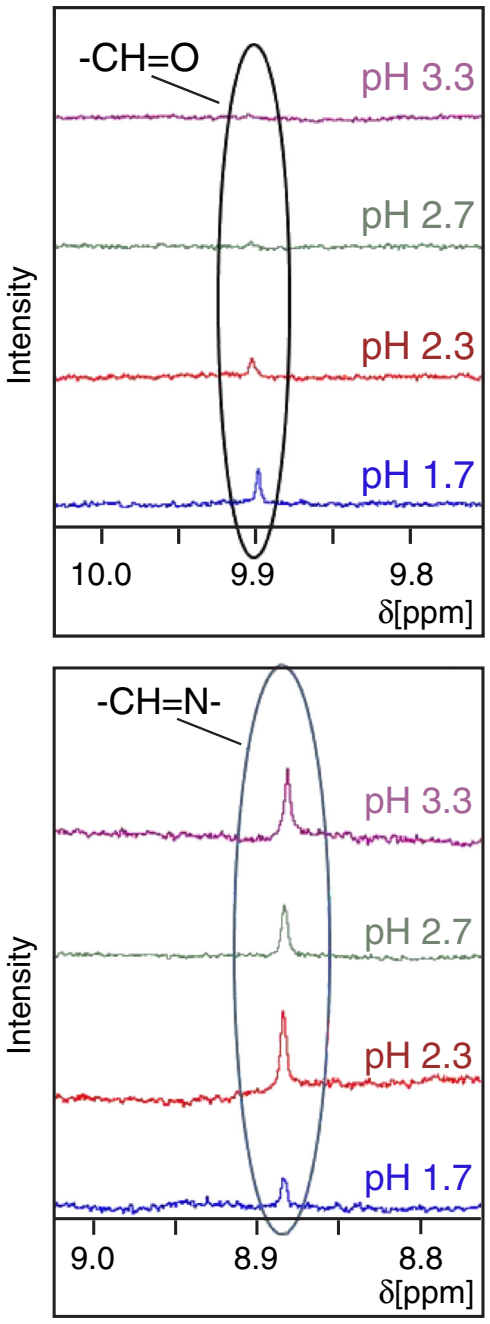

Fig. 5. NMR spectra of Ga–ME0163 solutions (1.19 mM Ga(III) and 1.17 mM L) at pH 1.7, 2.3, 2.7, and 3.3. The data point to the hydrolytic cleavage of −CH═N− of ME0163, producing the THB compound at pH < < 2.7, namely ~1 pH unit lower than in the absence of Ga(III).

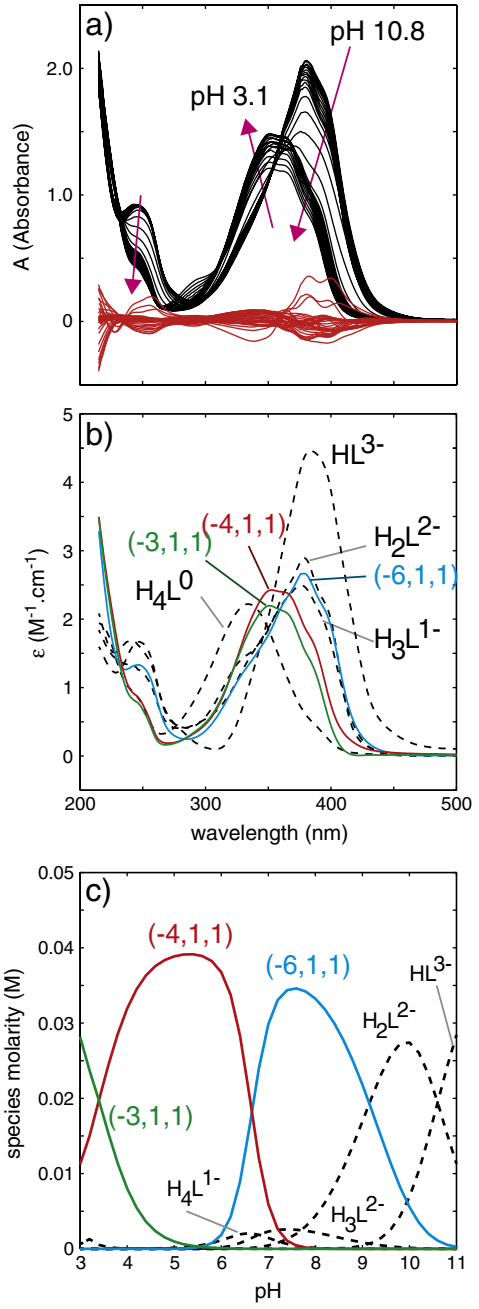

Fig. 6. a) Example of one of the two sets of spectrophotometric titrations of ME0163 in 0.1 M NaCl at 25 °C. Red arrows show changes in spectral intensity with decreasing pH. Red lines show deviations of fit of the model to the data (black lines). b) Molar adsorption coefficients of the two species responsible for the data in a) and related with the pK_a values of Table 1. Molar absorption coefficients of subsystem species are shown with dotted lines for comparison. c) Distribution of L species for 0.05 mM Ga (III) and 0.04 mM L. Green line represents $Ga(OH)_2H_3L^0$, red line $Ga(OH)_3H_3L^{1-}$ and blue line $Ga(OH)_3HL^{3-}$.

study, is much better at preventing $Ga(OH)_3$ precipitation at physiological pH [12] making it a very interesting candidate for biological studies.

3.4. Conclusions

In this study we have characterized the solution chemistry of the gallium hydrazone complex Ga–ME0163 and found that its strength of complex formation to Ga(III) is close to that of EDTA and only slightly less than DFOB. The complex formed exhibited enhanced stability at low pH compared with the pure ligand due to the binding of Ga(III) in the hydrazone motif blocking the site of acid-induced hydrolysis of the ligand. This speciation, as well as the stability of the Ga(III) complex, is of great importance to understand the biological activity of this complex and to be able to predict how its stability can be preserved in different types of conditions. Stability issues in the form of hydrolysis of the hydrazone bond have previously been identified as a problem for pharmaceutical usage [9] of these types of substances despite the promising biological effect and low toxicity profile for many of them. However, considering that the presence of metal ions such as Ga(III) dramatically increases the stability of these molecules at low pH, it could be worth re-examining them as candidates for drugs targeting bacterial virulence

and biofilm formation. Furthermore, since the complex formation between Ga(III) and the hydrazone is slightly lower than that of Ga-DFOB it can be expected that the complex would efficiently deliver Ga^{3+} to the bacterial cells making it a very interesting candidate for antibacterial drugs that would be active in Fe restricted conditions.

Abbreviations

ME0163	2-oxo-2-[*N*-(2,4,6-trihydroxy-benzylidene)-hydrazino]-acetamide
L	ligand
DFOB	desferrioxamin B
THB	2,4,6-trihydroxybenzaldehyde
OAH	oxamic acid hydrazide
Ka	the acid dissolution constant
β	overall formation constant
β_{pqr}	overall formation constant for reaction of reactants with stoichiometric coefficients *p*, *q*, and *r*
SOS	sum of squares of errors
K_{HC}	degradation constant
SVD	singular value decomposition
CTTS	charge-transfer-to-solvent

Acknowledgments

The Swedish Research Council is acknowledged for funding (#2011-3504 for M. Ramstedt; #2012-2976 for J.-F. Boily). The Kempe foundation is acknowledged for funding enabling purchase of the UV–VIS-NIR spectrometer used in this study (#SMK-1144). Prof Staffan Sjöberg is greatly acknowledged for valuable discussions and comments throughout the project and on the final manuscript. Ingegärd Andersson is greatly acknowledged for experimental help with titrations.

Appendix A. Supplementary data

Supplementary data associated with this article can be found in the online version, at http://dx.doi.org/10.1016/j.jinorgbio.2014.04.012. These data include MOL files and InChiKeys of the most important compounds described in this article.

References

[1] D.A. Rasko, V. Sperandio, Nat. Rev. Drug Discov. 9 (2010) 117–128.
[2] M. Dahlgren, C. Zetterström, A. Gylfe, A. Linusson, M. Elofsson, Bioorg. Med. Chem. 18 (2010) 2686–2703.
[3] D. Wang, C. Zetterström, M. Gabrielsen, K. Beckham, J. Tree, S. Macdonald, O. Byron, T. Mitchell, D. Gally, P. Herzyk, A. Mahajan, H. Uvell, R. Burchmore, B. Smith, M. Elofsson, A. Roe, J. Biol. Chem. 286 (2011) 29922–29931.
[4] A. Slepenkin, P. Enquist, U. Hagglund, L. de la Maza, M. Elofsson, E. Peterson, Infect. Immun. 75 (2007) 3478–3489.
[5] A. Layton, D. Hudson, A. Thompson, J. Hinton, J. Stevens, E. Galyov, M. Stevens, FEMS Microbiol. Lett. 302 (2010) 114–122.
[6] H. Chu, A. Slepenkin, M. Elofsson, P. Keyser, L.M. de la Maza, E.M. Peterson, Int. J. Antimicrob. Agents 36 (2010) 145–150.
[7] D. Richardson, L. Vitolo, G. Hefter, P. May, B. Clare, J. Webb, P. Wilairat, Inorg. Chim. Acta 170 (1990) 165–170.
[8] L. Vitolo, G. Hefter, B. Clare, J. Webb, Inorg. Chim. Acta 170 (1990) 171–176.
[9] Z. Kovacevic, Y. Yu, D.R. Richardson, Chem. Res. Toxicol. 24 (2011) 279–282.
[10] A.-M. Albrecht-Gary, S. Blanc, N. Rochel, A.Z. Ocaktan, M.A. Abdallah, Inorg. Chem. 33 (1994) 6391–6402.
[11] E. Becker, D.R. Richardson, J. Lab. Clin. Med. 134 (1999) 510–521.
[12] D.R. Richardson, Antimicrob. Agents Chemother. 41 (1997) 2061–2063.
[13] E. Banin, A. Lozinski, K.M. Brady, E. Berenshtein, P.W. Butterfield, M. Moshe, M. Chevion, E.P. Greenberg, Proc. Natl. Acad. Sci. U. S. A. 105 (2008) 16761–16766.
[14] O. Rzhepishevska, B. Ekstrand-Hammarström, M. Popp, E. Björn, A. Bucht, A. Sjöstedt, H. Antti, M. Ramstedt, Antimicrob. Agents Chemother. 55 (2011) 5568–5580.
[15] Y. Kaneko, M. Thoendel, O. Olakanmi, B. Britigan, P. Singh, J. Clin. Investig. (2007) 877–888.
[16] A.B. Kelson, M. Carnevali, V. Truong-Le, Curr. Opin. Pharmacol. 13 (2013) 707–716.
[17] D.R. Richardson, E.H. Tran, P. Ponka, Blood 86 (1995) 4295–4306.
[18] A. Despaigne, G. Parrilha, J. Izidoro, P. da Costa, R. dos Santos, O. Piro, E. Castellano, W. Rocha, H. Beraldo, Eur. J. Med. Chem. 50 (2012) 163–172.
[19] J. Gao, D.R. Richardson, Blood 98 (2001) 842–850.
[20] P.V. Bernhardt, P.C. Sharpe, M. Islam, D.B. Lovejoy, D.S. Kalinowski, D.R. Richardson, J. Med. Chem. 52 (2009) 407–415.
[21] O. Rzhepishevska, S. Hakobyan, B. Ekstrand-Hammarström, Y. Nygren, T. Karlsson, A. Bucht, M. Elofsson, J.-F. Boily, M. Ramstedt, J. Inorg. Biochem. 138 (2014) 1–8.
[22] P. Heinz-Helmut, UV-VIS Spectroscopy and Its Applications, Springer-Verlag, Heidelberg, 1992.
[23] J. Boily, T. Seward, J. Solut. Chem. 34 (2005) 1167–1190.
[24] J. Boily, T. Seward, J. Solut. Chem. 34 (2005) 1387–1406.
[25] P. Persson, K. Zivkovic, S. Sjöberg, Langmuir 22 (2006) 2096–2104.
[26] ChemAxon Ltd, https://www.chemaxon.com/products/marvin/ 2014 (Accessed 10th March).